

Small-angle x-ray scattering studies of tertiary folding of tRNA^{Phe}

Xingwang Fang¹, K. Littrell², X-j. Yang¹, S. Henderson³, S. Seifert⁴, P. Thiyagarajan², T. Pan¹, and T.R. Sosnick¹

¹Department of Biochemistry and Molecular Biology, The Univ. of Chicago, 920 East 58th Street, Chicago, IL 60637 USA

²Intense Pulsed Neutron Source, Argonne National Laboratory, 9700 S. Cass Ave., Argonne, IL 60439 USA

³Department of Physics, University of Colorado, Boulder, CO 80309 USA

⁴Chemistry Divisions, Argonne National Laboratory, 9700 S. Cass Ave., Argonne, IL 60439 USA

Introduction

The compaction of a tertiary RNA can be envisioned to occur in at least two steps. The initial formation of an independently stable secondary structure first brings two unstructured regions into close proximity. Subsequent formation of the tertiary structure could then bring secondary structural motifs together. Actual experimental information, however, is sparse on the relationship between compaction and other folding processes in tertiary RNA folding.

Small-angle x-ray scattering (SAXS) is useful for the characterization of unfolded and partially folded states that are not readily studied by high-resolution techniques such as NMR or crystallography. SAXS also is an effective method to follow changes in size and shape accompanying folding transitions.

SAXS was used to investigate the structure and Mg²⁺-dependent folding of the yeast tRNA^{Phe}. These studies were conducted at relatively low (μ M) RNA concentrations. These studies led to the relationship between compaction and other folding events, the nature of the unfolded and the intermediate forms, and the thermodynamics of tertiary RNA folding.

Methods and Materials

SAXS experiments were carried out at the anomalous SAXS instrument [1] on the BESSRC-CAT 12-ID beamline of Argonne National Laboratory's Advanced Photon Source (APS). Data were collected using a nine-element (15 cm x 15 cm) mosaic CCD area detector and exposure times were 1–6 seconds for each measurement. Sample to detector distance was 3 m and energy of x-ray radiation was set to 13.5 keV. Samples were injected into a flow cell consisting of motored syringes that can inject a known quantity of a solution into the 1.5 mm-diameter cylindrical capillary viewed by the x-ray beam. The background scattering was from a buffer solution in the identical configuration that enables proper background subtraction.

To reduce the possibility of radiation damage, the samples were measured under constant flow conditions in a thermostatically controlled 1.5 mm quartz capillary connected to a Hamilton (Reno, NV) electronic titrator. The Mg²⁺ titrations were performed using a second syringe that added aliquots of concentrated MgCl₂ solutions to a 0.5–1 ml sample followed by withdrawal through the quartz capillary.

Results and Discussion

For tRNA^{Phe}, the measured values for the radius of gyration (R_g , ~ 23.5 Å), the maximum dimension (d_{max} , ~ 80 Å), and the pair distance distribution function ($P(r)$) are very similar to that calculated from the crystal structure. Furthermore, the Mg²⁺-dependent folding transitions (unfolded-to-intermediate-to-native, or U-to-I-to-N) observed by SAXS (Figure 1) mirror those determined previously using chemical and spectroscopic probes. The R_g of the intermediate state of tRNA^{Phe} is about 30% larger than its corresponding native states. Although the I and N states of tRNA^{Phe} are compact and independent of urea concentration, the dimensions of the denatured state(s) are strongly dependent on solution conditions and can be highly extended in the presence of urea. The measured size and shape changes accompanying tertiary RNA folding transitions correlate well with the amount of surface buried, as characterized by the urea m-value. These SAXS results lend additional support to the applicability of a cooperative Mg²⁺-binding model for tertiary RNA stability. In summary, SAXS provides an excellent measure of compaction accompanying folding transitions of tertiary RNAs and is a powerful complement to other more frequently applied methods including optical spectroscopy, chemical modification, and functional assays.

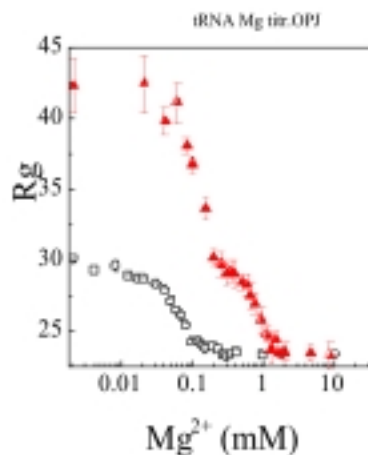


Figure 1: Mg²⁺ titration of 0.3 mg/ml YF0, 20 mM Tris (pH = 8.1), 37°C, APS.

Acknowledgments

This work was supported by grants from the NIH (R01GM57880 to T.P and T.R.S.), the Cancer Research Foundation (T.R.S), the U.S. Department of Energy, BES-Materials Science, under contract W-31-109-ENG-38 (P.T),

The University of Chicago-Argonne National Laboratory Collaborative Seed Grant Program (T.R.S. and P.T.), and the Packard Interdisciplinary Science Program (T.R.S., P.T., S. Berry, D. Lynn, and S. Meredith). Use of the APS was supported by the U.S. Department of Energy, Basic Energy Sciences, Office of Science, under Contract No. W-31-109-Eng-38.

Reference

[1] S. Seifert, R.E. Winans, D.M. Tiede, and P. Thiyagarajan, *J. Appl. Cryst.* (in press).